Accepted Manuscript

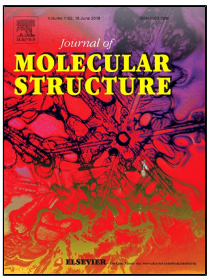

Different Chemical Behaviors and Antioxidant Activity of Three Novel Schiff bases Containing Hydroxyl Groups. X-ray structure of $CH_2\{cyclo\text{-}C_6H_{10}\text{-}NH{=}CH\text{-}(2\text{-}O\text{-}naphth)\}_2.H_2O$

Musa A. Said, David L. Hughes, Mohammed Al-Mamary, Nadia S. Al-Kaff, Wael S. Al-Harbi

PII:	S0022-2860(18)30384-3
DOI:	10.1016/j.molstruc.2018.03.089
Reference:	MOLSTR 25028
To appear in:	*Journal of Molecular Structure*
Received Date:	02 January 2018
Revised Date:	12 March 2018
Accepted Date:	22 March 2018

Please cite this article as: Musa A. Said, David L. Hughes, Mohammed Al-Mamary, Nadia S. Al-Kaff, Wael S. Al-Harbi, Different Chemical Behaviors and Antioxidant Activity of Three Novel Schiff bases Containing Hydroxyl Groups. X-ray structure of $CH_2\{cyclo\text{-}C_6H_{10}\text{-}NH{=}CH\text{-}(2\text{-}O\text{-}naphth)\}_2.H_2O$, *Journal of Molecular Structure* (2018), doi: 10.1016/j.molstruc.2018.03.089

Different Chemical Behaviors and Antioxidant Activity of Three Novel Schiff bases Containing Hydroxyl Groups. X-ray structure of $CH_2\{cyclo\text{-}C_6H_{10}\text{-}NH{=}CH\text{-}(2\text{-}O\text{-}naphth)\}_2.H_2O$

Musa A. Said[a*], David L. Hughes[c*], and Mohammed Al-Mamary[a], Nadia S. Al-Kaff[b], Wael S. Al-Harbi[a]

[a]Chemistry Department, College of Science, Taibah University, PO Box 30002, Code 14177, Al-Madinah Al-Munawarah, Kingdom of Saudi Arabia, [b]Biology Department, College of Science, Taibah University and [c]School of Chemistry, University of East Anglia, Norwich NR4 7TJ, U.K.

Dr. Musa A Said. E-mail: musa_said04@yahoo.co.uk
David L. Hughes. E-mail: D.L.Hughes@uea.ac.uk

Dedicated to Prof Dr. K. C. Kumara Swamy in honor of his 60th birthday.

The antioxidant activities of three new Schiff base compounds, **1 – 3**, were studied through their direct scavenging ability to eliminate free radicals using DPPH and ABTS methods and also through their indirect antioxidant activity as measured using the ferric thiocyanate (FTC) method. The number of OH groups in the compounds and their positions play a role in the activity. The crystal structure of $CH_2\{cyclo\text{-}C_6H_{10}\text{-}NH{=}CH\text{-}(2\text{-}O\text{-}naphth)\}_2.H_2O$ **(1),** has been determined and proves the existence of intramolecular hydrogen-bonds and hydrogen-bonded water molecules and reveals the keto-amine (N-H···O) tautomer of this compound. One *cyclo*-hexyl ring was found to be disordered, and was resolved in two orientations. Hydrogen atoms of the NH=CH groups were located in difference maps and were refined freely. Compounds **2** and **3** exhibit the enol-imine form. The UV-vis spectra of the three compounds have been studied in organic solvents of different polarity, and in basic and acidic media, and were found helpful in understanding the tautomeric forms in these compounds; the polarity was modified by adding (CF_3COOH) or [$(C_2H_5)_3N$] to the solvent. All three compounds have been characterized by elemental analysis, UV-vis, FTIR, NMR and MS.

Keywords: UV-vis, crystal structure; hydroxyl Schiff bases; intramolecular H-bonding and tautomers; antioxidant activities; DPPH, ABTS and FTC methods.

Introduction

The great importance of Schiff base compounds is due to their wide range of industrial applications and biological activities. They possess pharmacological activities such as antimicrobial, antifungal, anticancer, antiviral, anti-inflammatory, antiparasitic, antioxidant and more in industrial and auricular chemistry [1–4]. They also act as a basis for the synthesis of numerous organic compounds [5]. Schiff base compounds have an azomethine group (-CH=N-) which is made by the condensation of a carbonyl compound with a primary amine. It seems that this group is accountable for the biological activities demonstrated by a variety of Schiff bases [6]. Usually, Schiff bases synthesized from aromatic amines and aromatic aldehydes are stable and have an effective conjugation arrangement. Their biological activities can vary, depending upon the types of substituents attached to the aromatic rings [7]. The UV–vis spectra of 2-hydroxy Schiff bases have been studied in various nonpolar and polar solvents [8,9]. The band appearing at >400 nm is observed in various solvents including acidified solvents, and is responsible for the *keto*-amine form of the Schiff base [10]. In this study we report the synthesis and crystal structure of $CH_2\{$*cyclo*-C_6H_{10}-NH=CH-(2-O-naphth)$\}_2.H_2O$ (**1**) and the synthesis of compounds **2** and **3**, Scheme 1. We also describe the keto-amine, enol-imine, EE and ZZ forms of these novel compounds based on NMR, IR, UV-vis spectra and X-ray data. Interestingly, we aim here to demonstrate their potential antioxidant activities based on the position of the hydroxyl group in the Schiff base as shown in Scheme 1.

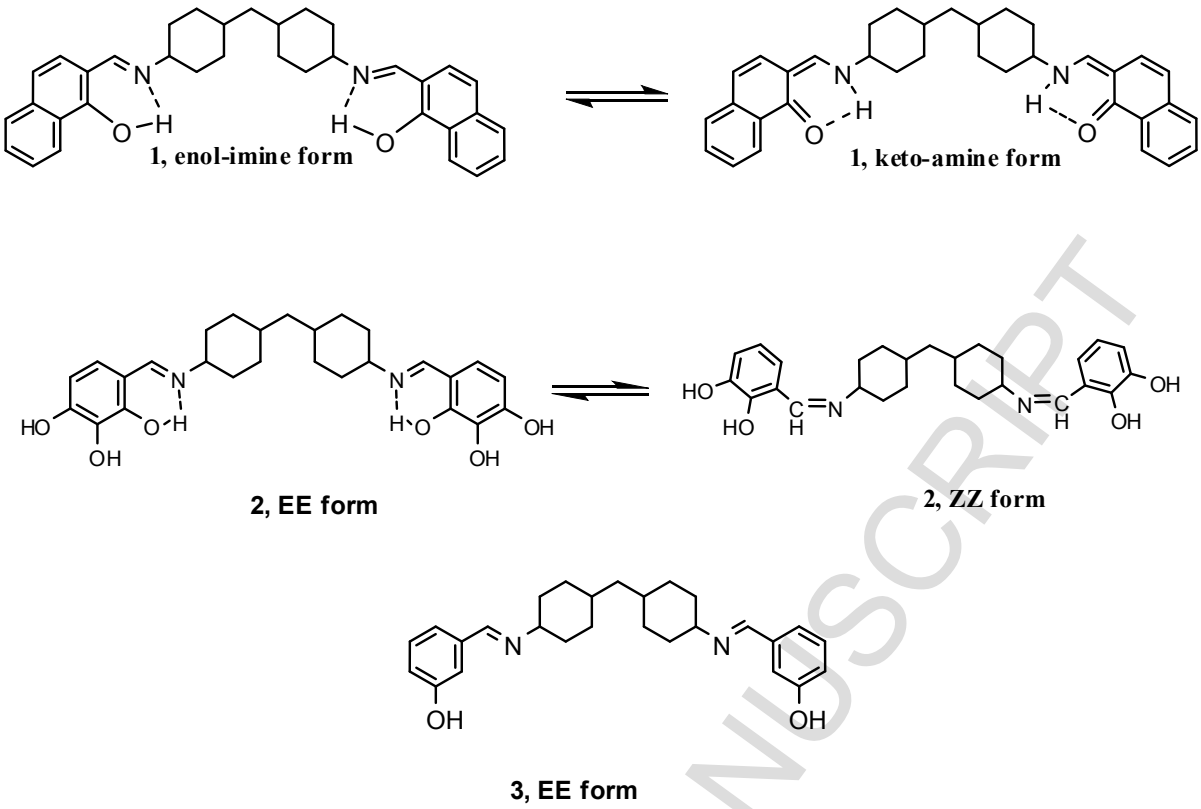

Scheme 1. Three different interesting forms found for compounds **1**, **2** and **3**.

Results and discussion

Schiff base compounds **1**, **2** and **3** were synthesized by a one-pot condensation reaction in dry ethanol, without the use of an acid as a catalyst, in good yields using a slightly modified, previously reported procedure [8, 9]. 4,4'-Methylenedicyclohexanamine was mixed with the aldehyde in 1:2 ratio in ethanol at room temperature, and the mixture was refluxed for two hours. The solvent was reduced to 1/3 and the product was allowed to form at room temperature. The products were re-crystallized from hot ethanol at room temperature. All **1**, **2** and **3** are solid and melt at 178, 210 and 183 °C respectively. The characteristic feature of the IR absorption bands of the free Schiff bases with the wave numbers 1639-1620 cm^{-1} corresponds to the C=N stretching vibration [10,13]. The delocalization in the π-electron pseudoaromatic six-membered ring (Fig 1), and the intramolecular hydrogen bonding may

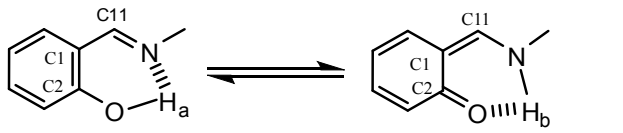

1, enol-imine form **1, keto-amine form**

Scheme 2. The possible pseudoaromatic six-membered ring involving H-bonding. Numbering corresponds to that in the X-ray structure.

have an effect on the keto-amine position [14]. Other expected vibration bands with the wave numbers in the 3440-3230 cm^{-1} region for *v* (OH, NH, H_2O, Ar-OH) for **1** and **2,** and *v*(OH, Ar-OH) for **3** were not observed due to the intramolecular H-bonding. Bands in the region of 3075-2920 cm^{-1} *v* (CH, H-Ar) were apparently observed for **1-3.** A small broad band for the second OH in compound **2** is clearer when compared to those for **1** and **3** due probably to the lack of involvement of the *m*-OH in the intramolecular H-bonding. The existence of intramolecular hydrogen bonding in **1** between the amine C=C-NH and the C=O (the keto-amine form) is further confirmed by the X-ray structure Fig. 2. The presence of C=O (^{13}C NMR *ca.* 177 ppm) in **1** and C=N (^{13}C NMR *ca.* 160 ppm) in **2** and **3** with possible intramolecular hydrogen bonding has been confirmed by FTIR. The UV-vis (maxima < 400 nm) and ^{13}C NMR spectra (no C=O band) confirm the enol-form only for **3**. The ^{1}H NMR spectrum for **3** shows one peak for OH downfield (9.31 ppm) indicating the presence of EE or ZZ form, Scheme 1. Probably, the EE form is more favored [12] due likely to steric hindrance. An interesting variation of ^{13}C NMR resonances for the carbons involved in the pseudoaromatic six-membered ring in Scheme 2 is presented in Table 1. The ^{1}H and ^{13}C NMR data (see Table1 and experimental section) of the compounds are in agreement with those

Table 1. ^{13}C and ^{1}H chemical shifts in ppm of the pseudoaromatic six-membered ring

Compound	**NHO or ArOH**	**CHN**	**C11**	**C1**	**C2**
1 (Keto and Enol)	14.95/14.35	9.21/9.18	158.16/157.76	125.90/125.64	177.58
2 (EE and ZZ)	14.57 (broad)	8.54/8.51	169.15	127.14/127.14	158.86/157.86
3 (EE or ZZ)	9.31	8.26	159.01	130.01	158.02

reported for the tautomeric forms of naphthaldimine **1** and salicylaldimine **2** and **3** Schiff bases in solution [9–13,15–17]. The tautomeric forms of the 2-hydroxy Schiff bases depicted by ^{1}H and ^{13}C NMR spectroscopy are drawn in Scheme 1. In $CDCl_3$ or DMSO-d_6, the ^{1}H NMR data for naphthaldimine show that both phenol-imine and keto-amine forms exist. The relative ratio of keto-amine/phenol-imine tautomers are estimated from the ^{1}H NMR spectrum of **1** in 2.32:1. In contrast, salicylaldimine compounds **2** and **3** show the existence of

only phenol-imine tautomers. Interestingly, both keto-amine and phenol-imine forms have been observed for derivatives **2** in basic media (see UV-vis study). However, both the salicylaldimines **2** and **3** show no keto-amine tautomer in either $CDCl_3$ and/or DMSO-d_6. For instance, no evidence has been observed for Ar=O in ^{13}C NMR for derivatives **2** and **3** in the region of 170-220 ppm, whereas this was not the case for derivative **1** (Table 1). Four signals, each appearing as a singlet, at 14.95, 14.35, 9.21 and 9.18 ppm can be ascribed to HC-N<u>H</u>, Ar<u>OH</u>, <u>H</u>C=N and <u>H</u>C=N respectively. The ^1H NMR integration indicates that the tautomeric equilibrium in **1** favors the phenol-imine form in both $CDCl_3$ and DMSO-d_6, showing N...H–O hydrogen bonding and likely EE form. Whereas, for salicylaldimine **2**, (Scheme 1) according to ^1H NMR spectra, two geometric isomers are possible (EE and ZZ). In contrast to **1** and **2**, compound **3** shows one geometric isomer (either EE or ZZ).

The potential energy barrier between the keto and enol form varies with the solvent polarity [4]. Hence, it is expected that the keto form is more dominant than the enol form in a polar solvent. Therefore, UV-vis spectra of the compounds were measured within 200-600 nm range in DMSO, ethanol, chloroform and benzene solvents. In this study, the UV-Vis spectra of **1**, **2** and **3** show mainly two maxima for the tautomeric forms of the 2-hydroxy Schiff base. A maximum appearing at more than 400 nm suggests that a keto form is present, while a maximum at less than 400 nm indicates that the enol form is present [18]. The characteristic UV–vis absorption bands of the compounds in DMSO, methanol, chloroform, THF and benzene are given in Table 2. There are three bands in the experimental spectra for **1** except for acidic and basic media, where there are two bands. Although **2** shows broad bands >400 nm in $CHCl_3$ and MeOH indicating the presence of the keto-amine form, a peak for C=O around 180 ppm in ^{13}C NMR could not be found. A highly interesting different chemical behavior of **1**, **2** and **3** in acidic and basic media is shown in Fig.2. Whereas **3** remains the same in both acidic and basic media, **2** changes in basic medium to show the keto-amine tautomer. It is quite obvious that **1** significantly favors keto-amine tautomer in acidic medium with respect to pure $CHCl_3$

Table 2. The results obtained from UV-vis analysis of compounds **1**, **2** and **3** in organic solvents, and acidic and basic media

Solvent	**λ (nm) for 1**	**λ (nm) for 2**	**λ (nm) for 3**
Benzene	248, 299, 426	248, 298	248, 299

THF	262, 310, 424	261, 308	261, 302
$CHCl_3$	248, 306, 419	249, 297, 425	249, 299
MeOH	260, 304, 423	264, 300, 428	260, 306
DMSO	265, 308, 421	259	264, 305
CF_3COOH, pH 3	294, 427	284	285
Et_3N, pH 9	307, 421	297	305

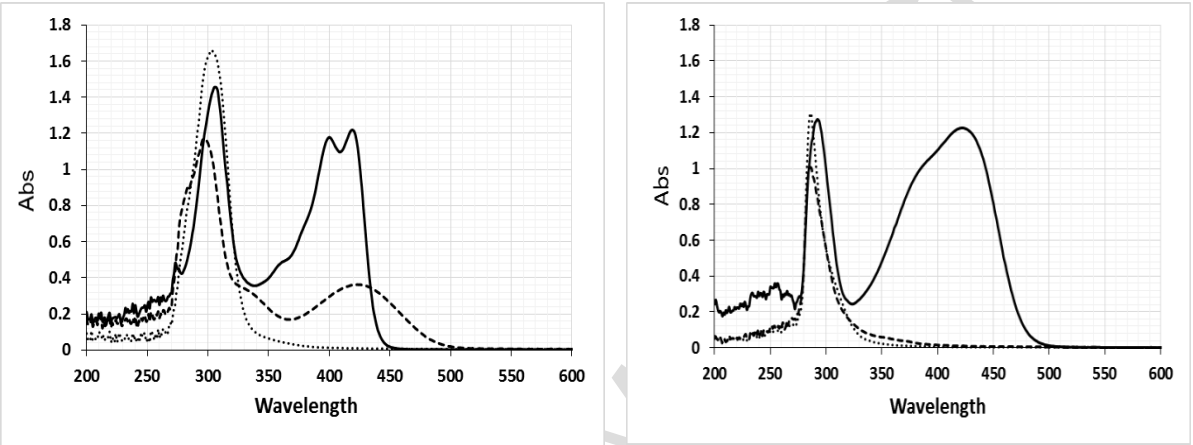

Fig. 1. UV-vis spectra for **1, 2** and **3** in acidic (right) and basic (left) media, with CF_3COOH, pH 3 and NEt_3 pH 9, respectively, added to the $CHCl_3$ solution. C = 5×10^{-5} M. **1**:——, **2**: ----, **3**: ·····

solvent as can be seen in Fig. 1. In general, bands around 350 nm are attributed to the π/π* transitions of –CH=N- group and n/π* transitions of the –C=O- group. It is noticed that as the solvent polarity increases, the keto/enol ratio increases, because the proton transfer can occur easily in acidic medium.

Experimental section

Chemicals were bought from Sigma-Aldrich. All commercial chemicals were used without further purification in open atmosphere and at room temperature. The melting points were taken on a Mel-Temp. Capillary melting point apparatus and are uncorrected. Carbon, hydrogen, nitrogen contents were estimated on a CHN Model CE-440 Analyzer and on an Elementar Vario EL III Carlo Erbo 1108. Infrared spectra (ν/cm^{-1}) were recorded on an IRAffinity-1S Shimadzu instrument, using KBr disks. MALDI mass chromatograms were

obtained on a Microflex Bruker instrument. ^{1}H- and ^{13}C-NMR spectra were recorded on a Bruker 400 MHz NMR Spectrometer at 293 K in $CDCl_3$ and DMSO-d_6. Spectra were internally referenced to TMS for $CDCl_3$. Peaks are reported in ppm downfield of TMS. The absorbance was measured on a Thermo Scientific Genesys 10s UV-vis spectrophotometer.

Compounds **1**, **2** and **3** were obtained in good yields following a published procedure [11,12]. The 4,4'-methylenedicyclohexanamine was mixed with the aldehyde in 1:2 ratio in ethanol (50 mL) at room temperature, and the mixture was refluxed for two hours. The solvent was reduced to 1/3 and the mixture was allowed to cool down to room temperature. The solid products were collected, dried under vacuum and characterized (Tables 1 and 3).

CH_2{cyclo-C_6H_{10}-NH=CH-(2-O-naphth)}$_2$ (1), keto-enol forms ratio, 1:2.31: ^{1}H NMR ($CDCl_3$): 14.95 (s, C-NH), 14.35 (s, Ph-OH), 9.21, 9.18 (CH=N), 8.12-6.72 (m, Ph-H), 4.41 (bs, N-CH), 3.93 (t, NCH), 3.55-0.98 (m, cyclohexyl-H and CHC$\underline{H_2}$CH). ^{13}C NMR (DMSO-d_6): 177.82, 177.58 (C=O, C=O.H_2O), 158.16, 157.73 (HC=N), 137.39-106.09 (aromatic), 60.25 (N-CH), 33.78-27.97 (cyclohexyl and CH$\underline{C}H_2$CH). FT-IR cm^{-1}**:** 3025, 2920, 2870, 1630, 1525, 1330, 1190, 850, 750. MALDI-MS: 519.41 [M^+]

CH_2{cyclo-C_6H_{10}-NH=CH-(3-OH-2-O-Ph)}$_2$ (2), EE to ZZ ratio 2.2:1: ^{1}H NMR (DMSO-d_6): 14.57 (b, Ph-OH), 8.54, 8.51 (CH=N), 6.83-6.58 (m, Ph-H), 3.68 (bs, N-CH), 3.26 (t, NCH), 1.86-0.93 (m, cyclohexyl-H and CHC$\underline{H_2}$CH). ^{13}C NMR (DMSO-d_6): 169.15 (HC=N), 158.86, 157.86 (C-OH), 127.29-122.02 (aromatic), 70.18, 66.39 (N-CH), 45.31-36.25 (cyclohexyl and CH$\underline{C}H_2$CH). FT-IR cm^{-1}: 3420, 3231, 2934, 2862, 1643, 1543, 1491, 1413, 1214, 1017, 893, 732. MALDI-MS: 451.20 [M^+]

CH_2{cyclo-C_6H_{10}-NH=CH-(3-OH-Ph)}$_2$ (3), EE or ZZ: ^{1}H NMR (DMSO-d_6): 9.31 (b,Ph-OH), 8.26 (CH=N), 7.24-6.84 (m, Ph-H), 3.14 (t, NCH), 1.79-0.97 (m, cyclohexyl-H and CHC$\underline{H_2}$CH). ^{13}C NMR (DMSO-d_6): 159.01 (HC=N), 158.02(C-OH), 138.17-144.07 (aromatic), 69.18, 66.66 (N-CH), 40.58-39.05 (cyclohexyl and CH$\underline{C}H_2$CH). FT-IR cm^{-1}: 3440, 2911, 2853, 1620, 1405, 1283, 1208, 565, 772, 678. MALDI-MS: 419.22 [M^+]

Table 3. Physical data for compounds **1**, **2** and **3**

No.	Amine (mmol)	Aldehyde (mmol)	Yield %	CHN analysis, Theo(actual)*	M.p °C

1	12.24	24.48	75%	81.05(80.89), 5.40(5.47)	7.38(7.41),	175-78
2	12.5	25.0	79.9	71.97(72.11), 6.22(6.33)	7.61(7.56),	205-210
3	10.46	20.92	86.3	77.48(77.39), 6.69(6.75)	8.19(8.08),	180-183

*Samples were subjected to vacuum under heating (oil bath, 50 ^{o}C) for two hours.

Structural commentary

Crystals of compound **1** were analysed by X-ray diffraction methods and have the structure shown in Fig. 2 and Fig. 3. Working out from the central methylene group of C(20), there are cyclohexyl groups in both directions; each of these has a chair conformation, with the bond from the central group in an *equatorial* arrangement in each case. From the ring of C(32-37), the C(32) – N(31) bond is *axial* and leads into an essentially planar NH=CH-(2-O-naphth) group. The hydrogen atoms on C(31) and N(31) were located clearly in trigonal planar positions and both were refined freely and well; there is a good N(31)–H(31a)…O(22) hydrogen bond which completes a planar six-membered ring with C(31,21,22). Bond dimensions in Table 4 in this ring indicate that C(31) = N(31) is a double-bond and C(22) – O(22) is too long to be a ketone bond. This indicates that this is a Zwitter-ion type group, with a positive charge on N(31) and a negative charge on O(22).

The cyclohexyl group of C(12-17), however, is disordered in two orientations, with a site ratio of 0.89:0.11. The C(12)-N(11) bond is common to both disorder components and is an *equatorial* bond from both component cyclohexyl rings. The remainder of this half of the molecule is very similar to that of the first half described above, *viz* good location and refinement of the H atoms on C(11) and N(11), formation of the N(11)-H(11a)…O(2) hydrogen bond and planar six-membered ring with C(1,2,11), similar short C(11) = N(11) and longer C(2) – O(2) bond lengths, and a similar Zwitter-ion system.

Table 4. Molecular dimensions. Bond lengths are in Ångstroms, angles in degrees. E.s.ds are in parentheses.

C(11)-N(11)	1.303(3)	C(31)-N(31)	1.307(3)
C(11)-H(11)	1.03(2)	C(31)-H(31)	1.02(2)
N(11)-C(12)	1.462(3)	N(31)-C(32)	1.467(3)
N(11)-H(11A)	0.97(3)	N(31)-H(31A)	0.93(3)
C(14)-C(15)	1.526(4)	C(35)-C(20)	1.523(3)

C(15)-C(20)	1.511(3)	C(35)-C(36)	1.538(3)
C(15)-C(16)	1.522(4)	C(22)-C(23)	1.430(3)
C(20)-C(35)	1.523(3)	O(9W)-H(9WA)	1.14(3)
C(22)-O(22)	1.291(3)	O(9W)-H(9WB)	0.91(4)
N(11)-C(11)-C(1)	123.5(2)	C(28)-C(27)-C(26)	121.0(2)
N(11)-C(11)-H(11)	114.4(12)	C(27)-C(28)-C(29)	121.5(2)
C(1)-C(11)-H(11)	122.1(12)	C(28)-C(29)-C(30)	117.4(2)
C(11)-N(11)-C(12)	123.7(2)	N(31)-C(31)-C(21)	123.7(2)
C(11)-N(11)-H(11A)	112.0(17)	N(31)-C(31)-H(31)	117.0(12)
C(12)-N(11)-H(11A)	123.9(17)	C(21)-C(31)-H(31)	119.3(12)
N(11)-C(12)-C(17)	108.4(2)	C(31)-N(31)-C(32)	124.4(2)
N(11)-C(12)-C(13)	109.89(19)	C(31)-N(31)-H(31A)	113.0(15)
O(22)-C(22)-C(21)	122.6(2)	C(32)-N(31)-H(31A)	121.9(15)
O(22)-C(22)-C(23)	119.6(2)	N(31)-C(32)-C(37)	111.51(18)
C(24)-C(23)-C(22)	120.9(2)	N(31)-C(32)-C(33)	109.1(2)
C(23)-C(24)-C(30)	123.2(2)	N(11)-C(62)-C(67)	129.0(10)
C(26)-C(25)-C(30)	121.5(2)	H(9WA)-O(9W)-H(9WB)	98(3)
C(25)-C(26)-C(27)	119.0(2)		

The oxygen atoms, O(2) and O(22), differ, however, in their intermolecular contacts; O(22) is the acceptor of hydrogen bonds from two water molecules, related about a centre of symmetry and which therefore also link up with O(22') of a neighboring molecule, Table 5, to form a hydrogen-bonded dimer. O(2) does not appear to have any close intermolecular contacts. Other short intermolecular contacts are at van der Waals' distances. Fig. 3 shows the dimer unit and neighboring molecules.

Table 5. Hydrogen bonds, in Ångstroms and degrees.

D-H...A	d(D-H)	d(H...A)	d(D...A)	<(DHA)
C(11)-H(11)...O(9W)#1	1.03(2)	2.29(2)	3.286(3)	163.7(17)
N(11)-H(11A)...O(2)	0.97(3)	1.75(3)	2.574(3)	141(2)
N(31)-H(31A)...O(22)	0.93(3)	1.77(3)	2.555(2)	140(2)
O(9W)-H(9WA)...O(22)	1.14(3)	1.66(3)	2.796(2)	179(3)
O(9W)-H(9WB)...O(22)#2	0.91(4)	1.98(4)	2.883(3)	171(4)

Symmetry transformations used to generate equivalent atoms:
#1 : x-1, y, z #2 : 2-x, 1-y, 1-z

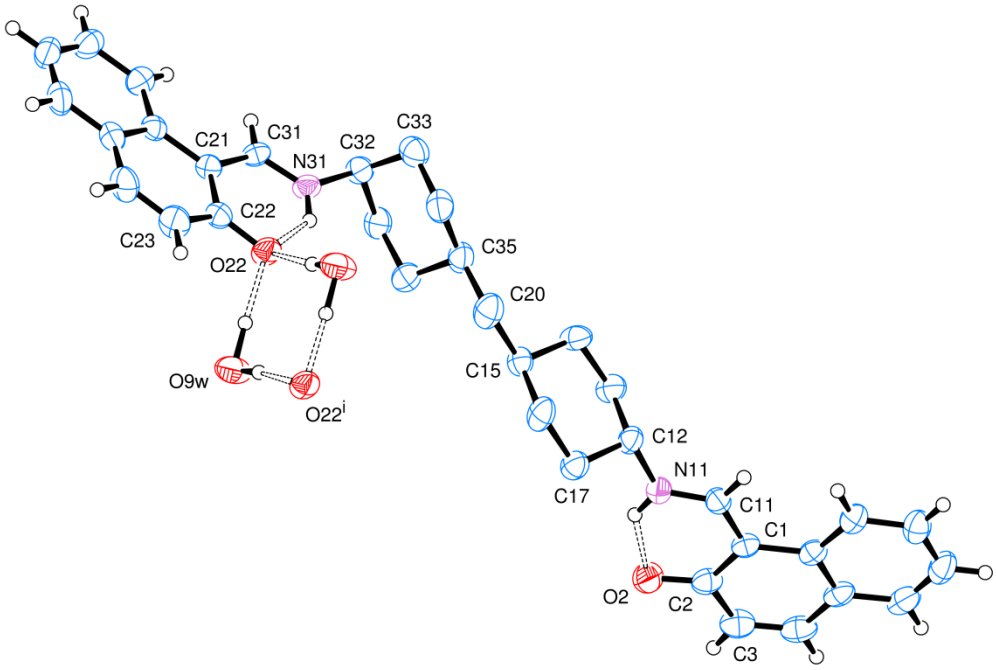

Fig. 2. View of the molecules of $CH_2\{cyclo\text{-}C_6H_{10}\text{-}NH{=}CH\text{-}(2\text{-}O\text{-}naphth)\}_2,H_2O$ (**1**), indicating the atom numbering scheme; the superscript i indicates the symmetry operation: 2-x, 1-y, 1-z. Hydrogen atoms (except for those involved in hydrogen bonds) and the minor component atoms of the disordered ring of C(12-17) have been omitted for clarity. Thermal ellipsoids are drawn at the 50% probability level.

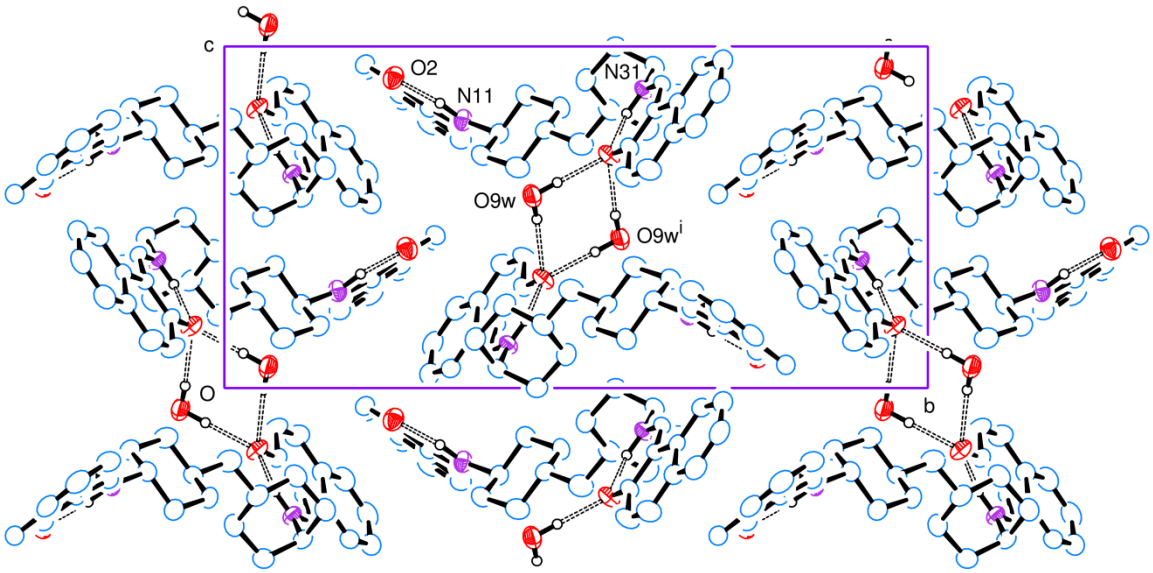

Fig. 3. View of the packing of compound **1** along the *a* axis.

Antioxidant investigation

The antioxidant activities of **1, 2** and **3** were investigated through their direct scavenging ability to remove free radicals using 1,1-diphenyl-2-picrylhydrazine (DPPH) and 2,2'-azinobis-(3-ethylbenzothiazoline-6-sulfonic acid (ABTS) methods [1,19] and also through their indirect antioxidant activity as measured using the ferric thiocyanate (FTC) method [1,20]. The direct ability of the synthesized compounds to neutralize free radicals ($DPPH^{\bullet}$ and $ABTS^{\bullet+}$) was monitored spectrophotometrically at 517 nm and 734 nm, respectively. Results shown in Table 6 indicate that **2** has the highest antioxidant activity as measured by each of the three methods.

Table 6. Antioxidant activity measurement using different methods

No.	Compound	DPPH	ABTS	FTC
1	**1**	19.21±1.11	73.00±8.08	50.00±2.20
2	**2**	85.11±1.52	89.80±1.14	70.07±2.65
3	**3**	40.66±5.63	87.58±1.01	67.47±0.80
P.C.	Vit. C	91.83±1.42	-	51.72±1.11
P.C.	Trolox	-	94.62±0.64	-

According to the DPPH method, **2** has very high antioxidant activity (85.11%), while other samples **1** and **3** show low (40.66%) to very low (19.21%) antioxidant activity, respectively. On the other hand, the results of antioxidant activity as measured by ABTS method were increased from 73.00 to 89.80 % in the order **2** > **3** > **1**, respectively. These findings could be attributed to the presence of hydroxyl groups attached to aromatic rings which might be responsible for the antioxidant activity of these Schiff bases. It is thus shown that **2,** containing two hydroxyl groups attached to each aromatic ring, has the highest antioxidant activities as measured by three methods (Table 6). It appears probable that this arrangement increases the conjugated systems and as a result increases the antioxidant activity of this compound. These results were in agreement with findings obtained by other researchers for compounds with di-hydroxy-phenyl groups [1,20]. The mechanism which occurs here could be similar to that which occurs in hydroxy chalcones and hydroxy flavonoid derivatives [21].
The indirect antioxidant activities of the synthesized compounds were measured using the ferric thiocyanate (FTC) method. This *in vitro* study measures the amount of peroxide produced during the initial stages of lipid peroxidation using linoleic acid. This method

mimics the process that occurs *in vivo*, where the presence of transition metals and high

No. of compound	Tyrosinase Inhibition (%)	Cholinesterase Inhibition (%)
1	25.42±1.77	65.98±6.29
2	21.72±0.35	79.05±4.39
3	32.33±1.07	35.75±2.20

concentrations of membrane-associated polyunsaturated fatty acids (PUFAs), under oxidative stress, largely act as triggers to initiate the process of lipid peroxidation (LPO). The new findings showed that the indirect antioxidant activity (the ability to prevent the Fenton reaction, $Fe^{2+} + H_2O_2 \rightarrow Fe^{3+} + HO^{\cdot} + HO^{-}$) of the tested compounds as measured by the FTC method was in the order **2** (70.07%) > **3** (67.47%> **1** (50.00%), respectively. Again, **2** showed the highest ability to prevent the formation of $HO^{\cdot}$ free radical, which is considered to be the most destructive free radical in biological systems.

The results in Table 7 show that the percentage inhibition of tyrosinase activities by our Schiff bases (**1**, **2**, and **3**) were very low (21.72- 32.33 %). Therefore, it is likely that none of these compounds can be used in cosmetics for whitening and depigmentation after sunburn.

Table 7. The effect of the synthesized compounds on tyrosinase and cholinesterase activity

On the other hand, the extent of inhibition of cholinesterase activity ranged from low to very high (35.75 to 79.05 %). Thus, the compound containing two hydroxyl groups attached to aromatic ring (**2**) can be considered as promising in the treatment of Alzheimer's disease (AD).

Biological activities

Enzyme inhibition:

a) The inhibition of acetylcholinesterase (AChE)

Inhibition of AChE was assessed by a slightly modified colorimetric method of Ellman *et al*. [22]. 2 mL PBS (Na_2HPO_3, 50 mM, pH = 7.7) and 0.1 mL of the Schiff base sample dissolved in DMSO (1mg/mL) were mixed in a test-tube. 0.3 mL of enzyme solution (0.005 U/mL) were added, and the mixture was incubated at 37 °C for 10 min. Then, 0.3 mL of acetylthiocholine iodide (0.5 mM, substrate) and 0.3 mL of DTNB (0.5 mM) were added.

After a further 30 min of incubation at 37 °C, absorbance was measured at 412 nm. Each sample was assayed in triplicate. Then: Inhibitory rate (%) = (Ac – At)/100.Ac, where Ac is the absorbance of control (without samples) and At is the absorbance in the presence of the Schiff base [22].

b) Tyrosinase activity assay

Tyrosinase activity assay was performed as previously described with modification [23]. The tyrosinase activity was measured using L-DOPA as a substrate. Samples dissolved in DMSO (1mg / mL), and L-DOPA (2 mM) in 50 mM Na_2HPO_4–NaH_2PO_4 buffer (pH 6.8) were incubated at 30 °C. Then, 2.8 mL L-DOPA was mixed with 0.1 mL sample. After 1 min, 0.1 mL of the aqueous solution of tyrosinase was added to the mixture and the absorbance was immediately monitored at 475 nm for 7 min. All measurements were performed in triplicate. The inhibitory rate was calculated according to the formula:

Inhibitory rate (%) = (Ac – At)/100.Ac, where Ac is the absorbance of control (without samples) and At is the absorbance in the presence of the samples [23].

Measurement of antioxidant activities

a) DPPH method

The assay was conducted following a previously described procedure with slight modification [24]. 2.0 mL of 0.3 mM DPPH solution was mixed with 0.1 mL of Schiff base dissolved in DMSO (1mg / mL). The mixture was then shaken vigorously and left for 30 min. in the dark. The absorbance was measured at 517 nm against a blank. Trolox was used as a positive control. These measurements were run in triplicate. The percentage of the scavenging activity is calculated:

Scavenging activity (%) = (Ac – As) /100.Ac, where Ac is the absorbance of DPPH without the test sample and As is the absorbance of DPPH in the presence of the test sample (or positive control).

b) ABTS method

This method was carried out as described by Arnao *et al.* [19], with slight modifications. A working solution was prepared by mixing equal volumes of 7.4 mM ABTS solution and 2.6 mM of potassium persulfate solution. This mixture was allowed to react for 14-16 h at room temperature in the dark to obtain $ABTS^{\bullet+}$. This solution was then diluted by mixing 1 mL of

$ABTS^{\bullet+}$ solution with 60 mL of phosphate buffer solution (pH = 7.4) to obtain an absorbance of 1.10±0.02 units at 734 nm using a UV/VIS spectrophotometer. This final $ABTS^{\bullet+}$ solution was prepared for each assay, in which 0.1 mL of Schiff base solution (1mg/mL in DMSO) was added to 3.0 ml of $ABTS^{\bullet+}$ final solution, incubated for 2 h in the dark before measuring the absorbance at 734 nm. Trolox (1mg/mL in DMSO) was used as a positive control [19].

c) FTC method

This method was used to study the inhibition of lipid peroxidation as described by Kikuzaki and Nakatani with slight modifications [25]. Into a 20 mL-vial with a screw cap, were transferred 4 ml of Schiff base (1 mg/ mL in DMSO), 4.1 mL of linoleic solution (2.51 %, in absolute ethanol), 8 mL of phosphate buffer (pH = 7), and 3.9 mL distilled water. This mixture was kept in an oven at 40 °C in the dark. This is the sample solution. 0.1 mL of the sample solution was transferred into a new 20 mL vial with a screw cap. 9.7 mL of 75% ethanol, 0.1 mL of ammonium thiocyanate (30 %) and 0.1 mL of ferrous chloride (20 mM in 3.5 % HCl) were added. After 3 minutes, the absorbance of the red colour was measured at 500 nm. Measurement of the absorbance was repeated at 24h intervals until one day after the absorbance of the control (without sample) reached maximum. Vit. C (1mg/ mL) was used as the positive control. The Inhibition (%) of lipid peroxidation was calculated:

Inhibition of lipid peroxidation (%) = (Ac – As) / 100.Ac , where As is the absorbance of the sample (or positive control) on the day when the absorbance of the control is maximum, and Ac is the absorbance of the control (without sample) on the day when it achieved its maximum [25].

Crystal structure analysis

Crystal data, data collection and structure refinement details are summarized in Table 8.

The structure was determined by the direct methods routines in the SHELXS program [27] and refined by full-matrix least-squares methods, on F^2's, in SHELXL [28]. The *cyclo*-hexanyl ring of C(12-17) was found to be disordered, and resolved, in two orientations. The non-hydrogen atoms (except for the minor component atoms of the disordered ring) were refined with anisotropic thermal parameters. Hydrogen atoms of the NH=CH groups and the

water molecule were located in difference maps and were refined freely and well; all remaining hydrogen atoms were included in idealized positions and their Uiso values were set to ride on the Ueq values of the parent carbon atoms.

Table 8. Crystal data and structure refinement for $CH_2\{cyclo\text{-}C_6H_{10}\text{-}NH{=}CH\text{-}(2\text{-}O\text{-}naphth)\}_2.H_2O$, **1**

Elemental formula	$C_{35}\ H_{38}\ N_2\ O_2,\ H_2\ O$
Formula weight	536.69
Crystal system, space group	Monoclinic, P $2_1/c$
Temperature	140(1) K
Unit cell dimensions	a = 12.1597(6) Å b = 22.1632(8) Å β = 101.859(5) ° c = 10.9781(6) Å
Volume	2895.4(2) $Å^3$
Z, Calculated density	4, 1.231 Mg/m^3
Radiation type	Mo Kα
μ (mm^{-1})	0.08
Wavelength	0.71073 Å
Crystal colour, shape	Colourless block
Crystal size	0.20 x 0.17 x 0.14 mm
Crystal mounting:	on a glass fibre, in oil, fixed in cold N_2 stream
Theta range for data collection	3.545 to 24.998 °
Data collection Diffractometer	Oxford Diffraction Xcalibur 3/Sapphire3 CCD diffractometer
Absorption correction	Multi-scan CrysAlis PRO, Agilent Technologies, Version 1.171.37.35 (2014) Empirical absorption correction using spherical harmonics, implemented in SCALE3 ABSPACK scaling algorithm
Tmin, Tmax	0.841, 1.000
No. of measured, independent and observed [I > 2σ(I)] reflections	40072, 5083, 3370
Rint	0.070
(sin θ/λ)max ($Å^{-1}$)	0.595
Refinement, R[$F^2 > 2\sigma(F^2)$], wR(F^2), S	0.054, 0.126, 1.04
No. of reflections	5083
No. of parameters	402
No. of restraints	2
H-atom treatment	H atoms treated by a mixture of independent and constrained refinement
Δρmax, Δρmin (e $Å^{-3}$)	0.37, −0.26

Computer programs: *CrysAlis PRO*, Agilent Technologies, Version 1.171.37.35 [26], *SHELXS97* [27] , *SHELXL* [28], *ORTEP* [29] and *WinGX* [30].

Conclusion

Antioxidant activities of the three Schiff bases were measured and it was concluded that the activities of these Schiff bases can be improved by introducing OH groups in their core

structure. The results of antioxidant activity as measured by ABTS method were increased from 73.00 to 89.80 % in the order **2** > **3** > **1**. Compound **2** has the highest antioxidant activity probably because it has two hydroxyl groups. From the title structure which reveals the keto-amine (N-H···O) tautomer and other characterization methods of the compounds, we conclude that salicylaldimines favor the enol form and naphthaldimines prefer the keto form. Acidic medium has a positive effect on the salicylaldimine and naphthaldimine forms which makes them favor the keto form, whereas basic medium did not have the same strong effect. The tautomeric equilibria of the Schiff bases have also been studied in polar and non-polar solvents by using mainly UV-vis and NMR data.

Supplementary data

CCDC 1813994 contains the crystallographic data for $CH_2\{cyclo\text{-}C_6H_{10}\text{-}NH{=}CH\text{-}(2\text{-}O\text{-}naphth)\}_2.H_2O$, compound **1**. These data can be obtained free of charge *via* www.ccdc.cam.ac.uk/data_request/cif or from the Cambridge Crystallographic Data Centre, 12 Union Road, Cambridge CB2 1EZ, UK; fax: (+44) 1223 336 033; or e-mail: deposit@ccdc.cam.ac.u.k. ~~Supplementary data associated with this article can be found, in the online version, at http://dx.doi.org/10.1016/j.poly.2013.08.015.~~

References

[1] M. Al-Mamary, S.I. Abdelwahab, H.M. Ali, S. Ismail, M.A. Abdulla, P. Darvish, Synthesis, antioxidant and antibacterial activities of some Schiff bases containing hydroxyl and methoxy groups, Asian Journal of Chemistry. 24 (2012) 4335–4339.

[2] P. Panneerselvam, R.R. Nair, G. Vijayalakshmi, E.H. Subramanian, S.K. Sridhar, Synthesis of Schiff bases of 4-(4-aminophenyl)-morpholine as potential antimicrobial agents, European Journal of Medicinal Chemistry. 40 (2005) 225–229. doi:10.1016/j.ejmech.2004.09.003.

[3] O.M. Walsh, M.J. Meegan, R.M. Prendergast, T. Al Nakib, Synthesis of 3-acetoxyazetidin-2-ones and 3-hydroxyazetidin-2-ones with antifungal and antibacterial activity, European Journal of Medicinal Chemistry. 31 (1996) 989–1000. doi:10.1016/S0223-5234(97)86178-8.

[4] A. Özek Yıldırım, M.H. Yıldırım, Ç. Albayrak Kaştaş, Keto-enol tautomerism of (E)-2-[(3,4-dimethylphenylimino)methyl]-4-nitrophenol: Synthesis, X-ray, FT-IR, UV–

Vis, NMR and quantum chemical characterizations, Journal of Molecular Structure. 1127 (2017) 275–282. doi:10.1016/j.molstruc.2016.07.117.

[5] R. Drozdzak, B. Allaert, N. Ledoux, I. Dragutan, V. Dragutan, F. Verpoort, Ruthenium complexes bearing bidentate Schiff base ligands as efficient catalysts for organic and polymer syntheses, Coordination Chemistry Reviews. 249 (2005) 3055–3074. doi:10.1016/j.ccr.2005.05.003.

[6] I. Vazzana, E. Terranova, F. Mattioli, F. Sparatore, Aromatic Schiff bases and 2 ,3-disubstituted-1 , 3-thiazolidin-4-one derivatives as antiinflammatory agents, Arkivoc. 5 (2004) 364–374.

[7] P.A. Vigato, S. Tamburini, The challenge of cyclic and acyclic schiff bases and related derivatives, Coordination Chemistry Reviews. 248 (2004) 1717–2128. doi:10.1016/j.cct.2003.09.003.

[8] G. Kaştaş, Investigating the prototropic tautomerism in (E)-2-[(4-fluorophenyl) iminomethyl]-5-methoxyphenol compound for solid state and solvent media by experimental and quantum computational tools, Journal of Molecular Structure. 1017 (2012) 38–44. doi:10.1016/j.molstruc.2012.03.005.

[9] H. Ünver, D.M. Zengin, K. Güven, Intramolecular hydrogen bonding and tautomerism in 1-[N-(4-bromophenyl)]aminomethylidene-2(1H)naphthalenone, Journal of Chemical Crystallography. 30 (2000) 359–364. doi:10.1023/A:1009521510428.

[10] H. Nazır, M. Yıldız, H. Yılmaz, M.N. Tahir, D. Ülkü, Intramolecular hydrogen bonding and tautomerism in Schiff bases. Structure of N-(2-pyridil)-2-oxo-1-naphthylidenemethylamine, Journal of Molecular Structure. 524 (2000) 241–250. doi:10.1023/A:1014347216821.

[11] L. Peng, C. Chen, C.R. Gonzalez, V. Balogh-Nair, Bioorganic studies in AIDS: Synthetic antifungals against *Pneumocystis carinii* based on the multivalency concept, International Journal of Molecular Sciences. 3 (2002) 1145–1161. doi:10.3390/i3111145.

[12] S. Bilge, Z. Kiliç, Z. Hayvali, T. Hökelek, S. Safran, Intramolecular hydrogen bonding and tautomerism in Schiff bases: Part VI. Syntheses and structural investigation of salicylaldimine and naphthaldimine derivatives, Journal of Chemical Sciences. 121 (2009) 989–1001. doi:10.1007/s12039-009-0128-2.

[13] H. Ünver, M. Yıldız, D.M. Zengin, S. Özbey, E. Kendi, Intramolecular hydrogen

bonding and tautomerism in N-(3-pyridil)-2-oxo-1-naphthylidenemethylamine, Journal of Chemical Crystallography. 31 (2001) 211–216. doi:10.1023/A:1014347216821.

[14] Z. Popović, V. Roje, G. Pavlović, D. Matković-Čalogović, M. Rajić, G. Giester, Preparation and characterization of the 1:1 adducts of mercury(II) halides with N-benzyl- and N-p-tolyl-2-oxo-1-naphthylideneamine. The crystal and molecular structures of two isostructural di-μ-halo-bis[halo(N-benzyl-2-oxo-1-naphthylideneamine)mercury(II)] adducts (halo=chloro, bromo), Inorganica Chimica Acta. 322 (2001) 65–73. doi:10.1016/S0020-1693(01)00542-4.

[15] D. A. Safin, K. Robeyns, Y. Garcia, Solid-state thermo- and photochromism in *N*,*N*′-bis(5-X-salicylidene)diamines (X = H, Br). RSC Advances, 2 (2012) 11379–11388. doi:10.1039/c2ra21631k.

[16] G.-Y. Yeap, S.-T. Ha, N. Ishizawa, K. Suda, P.-L. Boey, W.A. Kamil Mahmood, Synthesis, crystal structure and spectroscopic study of *para* substituted 2-hydroxy-3-methoxybenzalideneanilines, Journal of Molecular Structure. 658 (2003) 87–99. doi:10.1016/S0022-2860(03)00453-8.

[17] K. Wozniak, H. He, J. Klinowski, W. Jones, T. Dziembowska, E. Grech, Intramolecular hydrogen bonding in N-salicylideneanilines. X-ray diffraction and solid-state NMR studies, Journal of the Chemical Society, Faraday Transactions. 91 (1995) 77-85. doi:10.1039/ft9959100077.

[18] L. Özdemir, Y. Yılmaz, M. Sönmez, M. Akkurt, M.N. Tahir, Synthesis and Crystal Structure of a New Phthalonitrile and Its Phthalocyanines Bearing Diamagnetic Metals, Synthesis and Reactivity in Inorganic, Metal-Organic, and Nano-Metal Chemistry. 46 (2016) 110–117. doi:10.1080/15533174.2014.900790.

[19] M. Arnao, M., Cano, A., M. Acosta, The hydrophilic and lipophilic contribution to total antioxidant activity, Food Chemistry. 73 (2001) 239–244. doi:10.1016/S0308-8146(00)00324-1.

[20] M. Čačić, M. Molnar, B. Šarkanj, E. Has-Schön, V. Rajković, Synthesis and Antioxidant Activity of Some New Coumarinyl-1,3-Thiazolidine-4-ones, Molecules. 15 (2010) 6795–6809. doi:10.3390/molecules15106795.

[21] S.B. Nimse, D. Pal, Free radicals, natural antioxidants, and their reaction mechanisms, RSC Advances, 35 (2015) 27986-28006. doi:10.1039/C4RA13315C.

[22] G.L. Ellman, K.D. Courtney, V. Andres, R.M. Featherstone, A new and rapid

colorimetric determination of acetylcholinesterase activity, Biochemical Pharmacology. 7 (1961) 88–95. doi:10.1016/0006-2952(61)90145-9.

[23] L-H. Chen, Y.-H. Hu, W. Song, K.-K. Song, X. Liu, Y.-L. Jia, J.-X. Zhuang, Q.-X. Chen, Synthesis and antityrosinase mechanism of benzaldehyde thiosemicarbazones: Novel tyrosinase inhibitors, Journal of Agricultural and Food Chemistry. 60 (2012) 1542–1547. doi:10.1021/jf204420x.

[24] O.P. Sharma, T.K. Bhat, DPPH antioxidant assay revisited, Food Chemistry. 113 (2009) 1202–1205. doi:10.1016/j.foodchem.2008.08.008.

[25] H. Kikuzaki, N. Nakatani, Antioxidant Effects of Some Ginger Constituents, Journal of Food Science. 58 (1993) 1407–1410. doi:10.1111/j.1365-2621.1993.tb06194.x.

[26] Oxford Diffraction *CrysAlis PRO*. Oxford Diffraction Ltd, Yarnton, UK, (2011).

[27] G.M. Sheldrick, A short history of *SHELX*, Acta Crystallographica Section A, Foundations of Crystallography. 64 (2008) 112–122. doi:10.1107/S0108767307043930.

[28] G.M. Sheldrick, Crystal structure refinement with *SHELXL*, Acta Crystallographica Section C, Structural Chemistry 71 (2015) 3-8.

[29] C.K. Johnson, ORTEP II, Report ORNL-5138, Oak Ridge National Laboratory, TN, (1976).

[30] L.J. Farrugia, *WinGX* and *ORTEP* for Windows: An update, Journal of Applied Crystallography. 45 (2012) 849–854. doi:10.1107/S0021889812029111.